Journal of
Applied Crystallography
ISSN 0021-8898

Received 16 August 2006
Accepted 20 December 2006

Upgrade of the small-angle X-ray scattering beamline X33 at the European Molecular Biology Laboratory, Hamburg

Manfred W. Roessle,[a]* Robbert Klaering,[a] Uwe Ristau,[a] Bernd Robrahn,[a] Doris Jahn,[a] Thomas Gehrmann,[a] Petr Konarev,[a] Adam Round,[a] Stefan Fiedler,[a] Christoph Hermes[a] and Dmitri Svergun[a,b]

[a]EMBL Hamburg, Notkestrasse 85, D-22603 Hamburg, Germany, and [b]Institute of Crystallography, Russian Academy of Science, 119333 Leninsky pr., 59 Moscow, Russia. Correspondence e-mail: manfred.roessle@embl-hamburg.de

The small-angle X-ray scattering beamline X33 of the European Molecular Biology Laboratory (EMBL) at the DORIS III storage ring [Deutsches Elektronen Synchrotron (DESY) Hamburg] was used for more than two decades to study the structure of non-crystalline biological systems. During recent years the beamline's scope has changed and is now predominantly used to analyze solutions of biological macromolecules. Owing to renewed interest in solution scattering studies from the biological community, the workload on the beamline has steadily increased. A major upgrade of X33 was performed to improve the beamline stability and data quality, to shorten the measurement time and to ensure user-friendly operation. The upgrade involved all major components of the beamline, including the optical system (monochromator, mirror, slits, beam monitors), electronics, control and acquisition software, X-ray detector system and the sample environment. The upgrade improved the brilliance by a factor of about three and the measuring time was reduced by a factor of seven. The knowledge and experience gained during the implementation of the upgrades to X33, may aid the design process for the BioSAXS beamline to be constructed for the PETRA-3 facility at DESY.

1. Introduction

Small-angle scattering of biological molecules provides information about low-resolution structure and structural transitions of macromolecules in solution and as well as about the structural organization of bulk samples (fibres, tissues *etc*). One of the first small-angle X-ray scattering (SAXS) synchrotron beamlines for biological applications was X33 at the EMBL Hamburg Outstation on the DORIS storage ring (Koch & Bordas, 1983). The beamline is located on a bending magnet with a source size of 1.961×0.512 mm^2 (full-width at half-maximum; FWHM) and a source divergence of 0.438×0.0238 mrad^2. The initial purpose of the X33 beamline (Fig. 1*a*) was to provide high X-ray flux for time resolved muscle fibre diffraction and kinetic solution scattering experiments. X33 has been operating for over 20 years and the last major upgrade was in the mid 1980s and much of the beamline hardware and software has since become obsolete. Currently, most of the SAXS experiments at X33 are done on solutions of biological molecules. Novel data analysis methods developed for solution scattering during recent years (Svergun & Koch, 2003; Petoukhov & Svergun, 2003; Konarev *et al.*, 2006) have attracted a growing number of users to the beamline. They have obtained valuable information about the structure solution of macromolecules (*e.g.* Vestergaard *et al.*, 2005; Gherardi *et al.*, 2006). Owing to low sample concentration and low-scattering contrast between biological molecules and the surrounding solvent, the scattering signal from the particles under investigation may be less than one percent above the scattering from the solvent. The SAXS technique imposes high demands on beam stability, low-background scattering and requires detector systems with low-readout noise (Boulin *et al.*, 1988). Moreover, given the sensitivity of the biological samples to radiation damage and the steadily increasing user turnover, shorter measuring

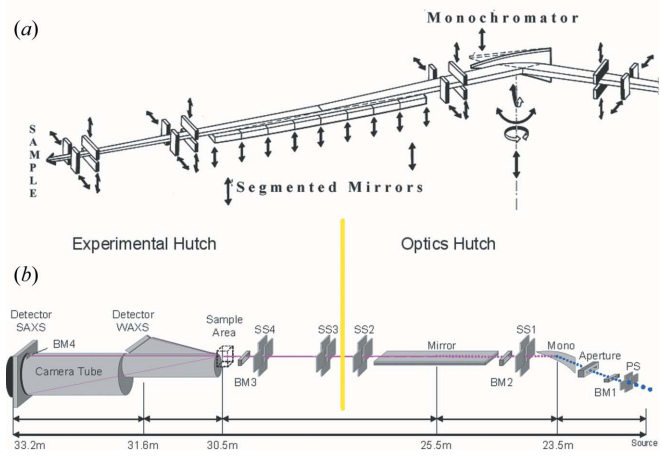

Figure 1
Outline of the optical setup of the X33 BioSAXS beamline before (*a*) and after the upgrade (*b*). PS is primary slits, SS1–SS4 are secondary slits and BM is a beam monitor.

times are of significant advantage in the SAXS experiments. For these reasons, we have performed a comprehensive upgrade of the beamline, including optics (Fig. 1*b*), electronics, detector, sample stage and acquisition system. This upgrade has permitted us to dramatically improve the parameters of the beamline providing a much more stable, fast and user-friendly operation for SAXS and WAXS (wide-angle X-ray scattering) experiments.

2. Upgrade of optical elements: monochromator, mirror, slits and shutter

2.1. Monochromator

Beam stability is one of the most important parameters in synchrotron scattering, especially for synchrotron solution SAXS. Small beam movements may produce noticeable background changes critical for the subtraction of solvent scattering. Originally the beamline was designed for high flux X-ray experiments using a horizontally diffracting and focusing triangular Si 111 monochromator at a fixed wavelength $\lambda = 0.15$ nm. The device is used as monochromator and also, by bending the crystal blade, for horizontal focusing. As a result, the fixed exit angle of the monochromator constrains the beamline geometry and cannot be changed. We have however modified the design of the monochromator to improve its thermal stability. The DORIS III storage ring at DESY operates at an injection-to-injection time of about 8 h with a typical current of 140 mA just after injection and approximately ~100 mA at the run end. The change in the current and thus in the white beam intensity leads to a variable heat load on the optical elements. Especially, the crystal monochromator as the first optical element is exposed to the white beam and therefore subject to large temperature changes. The previous monochromator design (water cooling *via* a plate fixed at its base) induced systematic horizontal movements of the focused beam during each synchrotron run. The observed movements were the result of the reduction in heat load over time which caused changes in the shape of the crystal due to its thermal expansion properties. To stabilize the operation an efficient cooling mechanism had to be implemented ensuring temperature stability in the large heat range. Since the Si 111 crystal has to be flexible for horizontal focusing, cooling through fixed contacts on either surface was not possible. Instead, an efficient cooling of the crystal blade was achieved using a bath of liquid metal [eutectic mixture of gallium, indium and tin (galinstan; Geratherm Medical AG, Geschwenda, Germany)], embedded in a water cooled metal block (Fig. 2). A thermocouple attached to the upper edge of the non-reflective side of the crystal allows the crystal temperature to be monitored directly. The monochromator and cooling system is mounted on a rotation stage allowing vertical translation, with an inclination table to control the tilt angle of the crystal blade with respect to the incident beam plane. The maximal footprint of the white beam on the crystal is limited by a fixed, water cooled, aperture of 4×10 mm centred at the geometrical centre of the crystal, which is placed 200 mm upstream the triangular crystal blade. A motor driven stage allows fine tuning of the rotation angle and the optional possibility of an active feedback is provided by a piezo stack actuator (Piezosystems, Jena, Germany). With the new setup, the temperature of the crystal ranges from 297 K without the beam to about 318 K under full flux conditions (140 mA ring current), and no systematic beam movements caused by the ring current decay are observed.

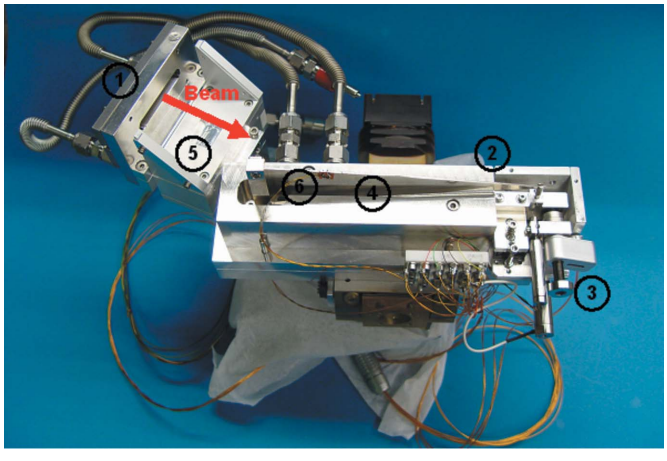

Figure 2
The X33 triangular monochromator setup. The beam aperture (1) limits the white beam footprint on the Si 111 blade (4). The crystal is cooled by a bath of liquid metal embedded in the water cooled metal block (2) and a bending mechanism (3) facilitates the focusing. A diode monitors the back scattering of a beryllium foil serving as a white beam monitor (5) (Be foil dismounted). A PT100 temperature sensor is mounted on the rear side of the crystals (6).

2.2. Gravimetrical U-bending rhodium coated X-ray mirror system

The second optical element is an X-ray mirror used for both vertical focusing and rejection of the higher harmonics. The original mirror of X33 (eight quartz segments each 200 mm long), was difficult to adjust, resulting in poor focusing with stray scattering in the vertical direction (Fig. 3). This mirror was replaced by a single 1000 mm rhodium coated U-bending mirror manufactured by SESO (Aix-en-Provence, France). In order to avoid beam instability due to temperature changes a zero thermal expansion coefficient ceramic (Zerodur) was chosen as the substrate material. The gravimetrical bending mechanism allows adjustments of bending radii from infinity down to 2 km. At a 4.5 mrad incident angle, the rhodium coating provides approximately 90% reflectivity at the fundamental wavelength and sufficient suppression of higher harmonics, confirmed by scattering patterns. The surface quality of the mirror was verified from NOM(nano optic measuring machine)-autocollimator measurements by the metrology group of BESSY (Berliner Elektronenspreicherring). Slope errors of 0.13 arcsec (0.04 arcsec in the middle section) were found. The bending radius of the mirrors is adjusted by a stepping motor, which is encapsulated in an argon atmosphere. The focal length can be varied down to 7 m (~2.3 km bending radius). The mirror was bought as a turn-key device and was placed in the existing mirror vacuum tank using a three point kinematic mount. The reflecting angle of the mirror is controlled by two lifting columns, one at each end of the mirror. The new mirror

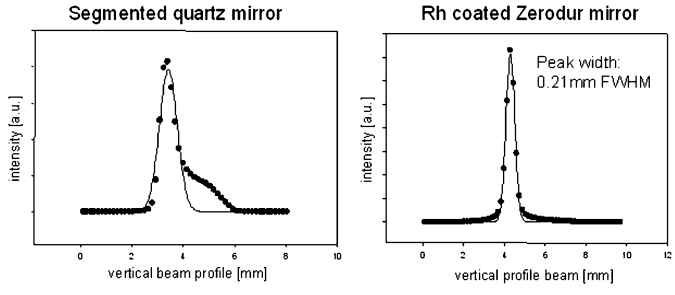

Figure 3
Beam profiles (FWHM, open slits) of the X33 BioSAXS beamline of the old and the new mirror. The vertical beam brilliance was enhanced by a factor of 1.7 and the asymmetric beam deformation disappeared.

improves the vertical focusing and reduces the vertical spot size from 0.35 mm to 0.21 mm (FWHM; see Fig. 3). Together with improvements in the reflectivity of the monochromator and of the mirror, the total increase in brilliance compared with the previous system is approximately a factor of three.

2.3. Slits

The slit systems of X33 are grouped units of four individual blades antagonistically paired to cut the beam in both the vertical and horizontal directions. Each blade is constructed of tungsten with a beam cutting edge at an angle of 5° with respect to the beam. The first pair of slits (primary slits, PS) are water cooled and define the white beam size on the crystal monochromator. The second pair (SS1, secondary slits) control the beam acceptance of the mirror and the third pair (SS2; positioned just after the mirror) cut out the stray radiation. In the previous X33 setup, there was only one slit system (SS3) downstream from SS2 positioned just before the sample. In the previous setup it was difficult to effectively cut the beam without introducing parasitic scattering. To improve beam size definition and minimize parasitic scattering, the sample position was moved 1.5 m downstream and another slit system (SS4) was introduced as displayed in Fig. 1(*b*). This allows SS3 to be used as beam forming slits and SS4 as guard slits solely to cut parasitic scattering.

2.4. Zero current X-ray shutter system

For the foreseen change of the detector a synchronized shutter system had to be implemented. This shutter opens during exposure and closes for the online readout of the image plate detector independently of the beamline safety shutter. For background reduction the system has to be operated in a vacuum and has to permit opening times from a few seconds to several minutes. Standard magnetic driven shutter systems are not suitable for vacuum operation because of overheating during longer opening times. Unlimited opening times can be achieved by a zero current shutter system developed inhouse (see Fig. 4). The zero current shutter system is operated by two pull action solenoids mounted antagonistically. When the solenoids are activated (using only short current pulses) one solenoid's core is pulled from a permanent magnet and the counterpart core is drawn towards (and held on) another magnet. As the shutter is held in place in the open or closed position by the permanent magnets, current is only required when the shutter is opened or closed. The bidirectional movement is synchronized with the detector by an electronic trigger signal. The X-ray beam is stopped by a lead reinforced aluminium plate in the closed position and the deadtime for opening/closing is 30 ms.

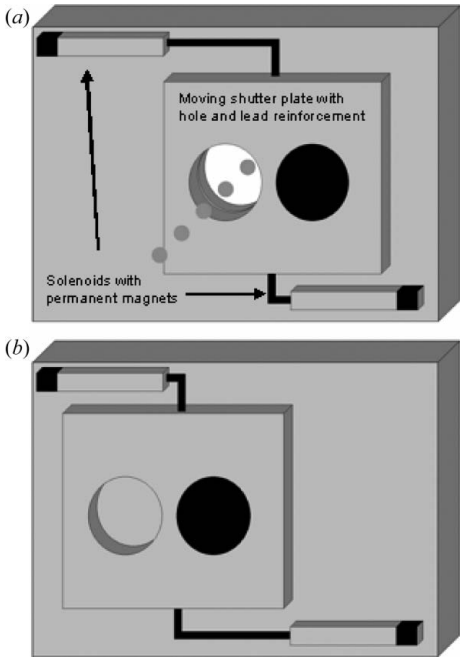

Figure 4
Zero current X-ray shutter for unlimited opening times, shown in (*a*) open and (*b*) closed positions.

3. MAR345 image plate SAXS detector

The upgrade of the optical system increased the brilliance and reduced the background scattering. Subsequently a suitable detector system had to be provided ensuring reduced exposure times and better data statistics. An optimal SAXS detector should allow recording data with low intrinsic background, high count rates and medium to fast readout (Berry *et al.*, 2003; Plaisier *et al.*, 2003; Nakamura *et al.*, 1997). All of the existing two-dimensional X-ray detectors such as CCD based devices, wire gas-chamber detectors or image plate readers have their advantages but also shortcomings for SAXS [see Plaisier *et al.* (2003) for a review]. The online image plate reader MAR345 from MarResearch appears to be a reasonable compromise combining a low intrinsic background and a large active area with the capability to record high local count rates. Its major disadvantage is the slow readout speed of the online scanner (about 90 s for scanning and about 60 s for erasing), which does not permit fast kinetic experiments. However, the MAR345 is a good choice for static experiments and slow kinetics. In the standard configuration of X33, the detector is vertically offset such that the beam centre is near the upper edge of the circular image plate. This allows one to record the broad range of the modulus of the scattering vector s ($s = 4\pi\sin\theta/\lambda$, where θ is the scattering angle) in one setting, *e.g.* from $s = 0.08\ \mathrm{nm}^{-1}$ to approximately $5\ \mathrm{nm}^{-1}$ at a sample-detector distance of 2.7 m. Using this configuration, most solution scattering experiments can be performed with this standard setup. This allows more efficient use of the measurement time and also saves the (usually limited) biological material. In the case when the data are required at higher resolution, simultaneous collection of WAXS data is possible on a linear gas detector mounted at about 1.2 m from the sample (Fig. 1*b*). This detector registers the photons scattered in the upper vertical direction and provides a range $s = 3\ \mathrm{nm}^{-1}$ to about $9\ \mathrm{nm}^{-1}$, which overlaps with the SAXS pattern of the MAR345. In Fig. 5(*a*) a comparison between a SAXS pattern recorded with a one-dimensional gas-filled wire detector employed earlier at X33 (15 min total exposure) and with 3 min exposure on a MAR345 (the latter after radial average, see Software section) is presented.

4. CANbus beamline electronics

During the beamline upgrade new control electronics were implemented replacing the outdated CAMAC system used at X33 previously. Typically beamline electronics have to operate different distributed modules for driving stepping motors, encoder value reading, transforming analogue values and recording digital signals. In particular, analogue signals are recorded at different positions on the beamline and have to be evaluated by a control system. Such a distributed signal recording can be handled by modern fieldbus systems where the recorded signal of a sensor is directly transformed

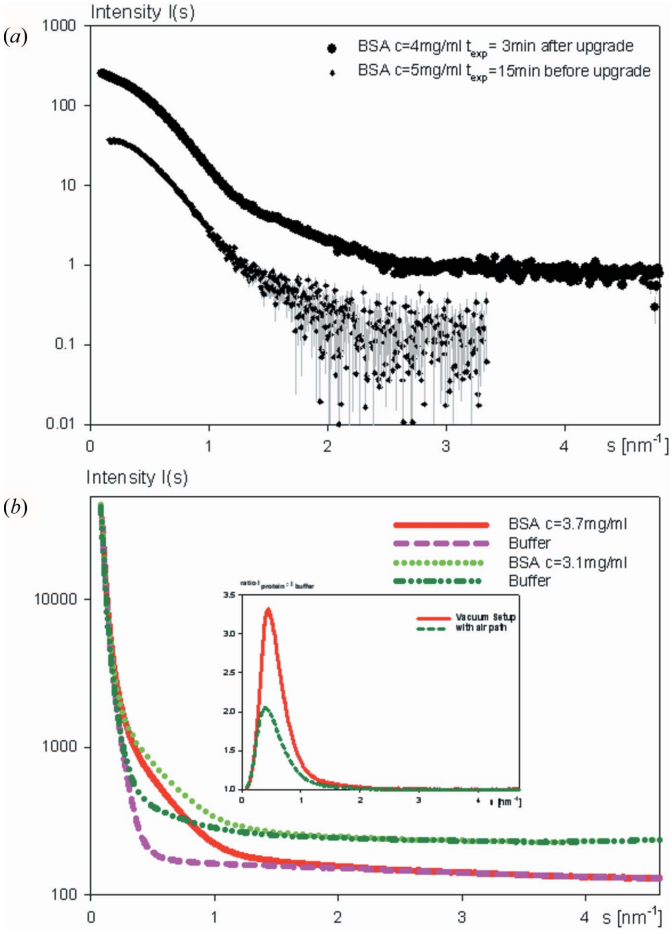

Figure 5
Signal improvement due to the beamline upgrade. (*a*) Improvement of the scattering pattern of BSA (bovine serum albumin) in buffer solution. The enhancement of data statistics, reduction in exposure time and extension in *s*-range after the upgrade of the monochromator, slit system, mirror and detector of the new setup (upper line) and the old setup (lower line) are clearly stated (data not scaled for intensity or protein concentration). (*b*) Comparison of sample and background raw data for the vacuum setup and air gap setup. Further improvement of the background noise and the signal to background ratio ($I_{\rm protein}$: $I_{\rm buffer}$ small inset) is achieved by introducing the vacuum cell setup.

into a digital signal and sent over the bus to a master control computer. Modern fieldbus systems (Lawrenz, 1997; Zeltwanger, 2001; Cena *et al.*, 2001) are able to bridge cable lengths up to 1000 m using standardized industrial components available from a number of different companies. Advanced error handling, heartbeat analysis and time stamping are additional features of modern fieldbus systems. The CANbus based CANopen protocol (Benoit *et al.*, 2006; Cena *et al.*, 2001; Farsi & Ratcliff, 1998; Zeltwanger, 2001) implemented at X33 is able to operate 42 independent stepping motors (30 of them are currently used) and the readings of 16 different encoder values for the motor feedback. A further 25 analogue/digital inputs for diode beam monitors and temperature sensors are foreseen.

5. Beamline control and data acquisition software

The software for beamline control and data acquisition on user dedicated experimental facilities is often operated by inexperienced visitors. The beamline computers and user dedicated programs at the beamline X33 were completely redesigned and adapted to the user

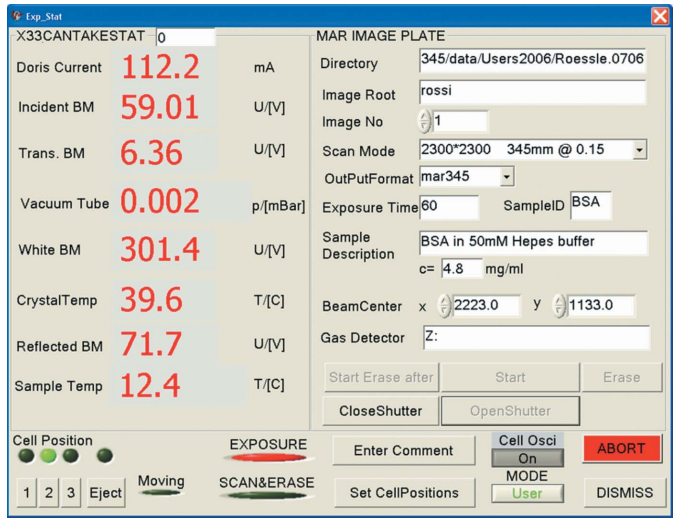

Figure 6
Graphical user interface (GUI) for experiment control. Important beamline parameters are displayed and experiment settings can be changed easily.

needs in the beginning of the upgrade. Further hardware and software changes during the beamline upgrade were implemented without changing the look-and-feel of the graphical user interface (GUI). This GUI displays all important beamline parameters such as white beam monitor, monochromatic beam monitor, incident flux monitor and transmitted flux measured at a pin diode mounted in the beamstop (Fig. 6). The temperatures of the monochromator crystal, of the specimen and the pressure in the detector tube are displayed as well. The MAR345 detector is operated directly from this system so that the entire measurement sequence can be conveniently performed from the same GUI. Relevant parameters such as exposure time, image file name conventions and sample description are set in the GUI, and transmitted to the MAR operating program, which triggers the data acquisition by opening the experimental shutter. All relevant parameters are stored in header files associated with MAR image files and they are extracted during data analysis for intensity normalization (transmitted flux and sample concentration) by the data reduction program *AUTOMAR*. This program performs the radial averaging of the two-dimensional files with respect to the beam centre and transforms them into one-dimensional files of scattering intensity *versus* angular axis in *s*-scale. The beam centre, averaging mask and the *s*-axis are generated for the given setup from the scattering patterns of silver behenate powder using the program *FIT2D* (Hammersley, 1998). The *AUTOMAR* program runs in the background of the data collection and waits until a new raw experimental data file emerges for it to be radially averaged. For a more detailed description of *AUTOMAR* and other programs in the data pipeline of X33 see Petoukhov (*et al.*, 2007). For simultaneous SAXS/WAXS measurements the GUI also starts the data acquisition on the linear WAXS detector using the batch mode of the linear gas detector data collection (National Instruments interface program written by F. Golding).

As the image plate is not a discrete photon counting detector it possesses an intrinsic noise ('dark current'), which influences the background subtraction accuracy. In systematic measurements a variation of the intrinsic noise between 3–4 counts per channels was found. Such variations already lead to systematic deviations during background subtraction, especially at higher scattering angles. To correct for the detector noise a portion of the image plate is masked out by a lead plate and this shielded area is used to evaluate the dark

current level for the given frame. This dark current correction has been incorporated into the *AUTOMAR* program and is done without user intervention.

The sample temperature is controlled by a Huber 125w thermostat allowing measurements in the range 248–473 K (usually 268–353 K), which is operated from a LabView interface. A workbench for sample handling is provided with an analytical balance, mini-centrifuge (Eppendorf), a Nanodrop ND-1000 spectrophotometer and a set of pipettes such that routine preparations of the biological samples can be performed at the beamline.

6. A vacuum cell for background reduction

As already stated, SAXS on biological macromolecules in solution requires that the background scattering be as low as possible. If the sample cell is situated in air (as was the case for the previous setup on X33) the scattering from the air itself contributes significantly to the background, therefore, it is advantageous to use a sample cell mounted in a vacuum (Dubuisson *et al.*, 1997). For solution scattering, working in a vacuum is not trivial as the sample container must be vacuum tight while ensuring an easy sample exchange. Capillary cells as used at some undulator SAXS beamlines (*e.g.* ID02 at European Synchrotron Radiation Facility, ESRF, Grenoble, or BioCAT at Argonne National Laboratory, Argonne) are less feasible for X33 because of its relatively large vertical beam size. Thus, a special flat cell was developed with thin X-ray transparent mica windows (20 µm). The cell is embedded in a temperature controlled holder block and sealed by O-rings. Reproducible bubble-free filling of the sample cell from outside the vacuum is achieved through a specially designed channel (diameter 0.6 mm), which fills the oval $6 \times 3 \times 1$ mm^3 ($w \times h \times t$) sample compartment from the bottom corner. The air displaced by the sample solution during filling is free to flow through the outlet situated at the top corner of cell (on the opposite side to which is it filled). The sample and cleaning solutions also exit the cell through the outlet pushed by a small overpressure. Standard Hamilton syringes are employed for all filling and washing operations, monitored by a TV camera (the cell image is reflected onto the camera by a turnable mirror). The filling volume of the vacuum cell (40 µl) is about half the volume of the in-air cell previously in operation on X33. Most importantly, the first test measurements with the vacuum setup revealed a significantly improved signal-to-background ratio, as illustrated in Fig. 5(*b*).

7. Conclusions

The upgrade of the X33 beamline at the EMBL Hamburg Outstation was aimed at improving its performance and user friendliness primarily for solution scattering studies of biological macromolecules. All components of the beamline were replaced or modernized and it currently provides a stable focal spot on the detector of FWHM of about 1×0.2 mm ($h \times v$) while maintaining the high flux of the original X33 setup (about 5×10^{11} photons s^{-1}). The typical measurement time is reduced from 15 min to 2 min, and with the low background vacuum cell, the sample volume required is 40–50 µl. These operation parameters can be considered good for a bending magnet beamline on a second generation source. The use of a large MAR345 image plate SAXS detector allows data to be recorded over a wide dynamic range (from about 80 nm to 1.3 nm resolution), *i.e.* most of solution scattering measurements can be done without changing the camera length. WAXS data (up to about 0.7 nm resolution) can be simultaneously measured by a linear gas detector. The beamline electronics were changed from CAMAC to the fieldbus CANbus with CANopen protocol allowing modular recording of all analogue values and control of the beamline stepping motors over a single signal line. The graphical user interface was newly designed and adapted to the needs of inexperienced beamline users. The experimental data are automatically reduced and processed [as described by Petoukhov *et al.* (2007)]. Importantly, some of the hardware and software solutions tested and implemented on X33 may become useful in the design and construction of the planned BioSAXS beamline at the upgraded PETRA-3 source at DESY. Thus, the CANbus system is one of the possible standards to be adopted for PETRA-3, and the experience gained from X33 will help in implementing a fieldbus on PETRA-3 beamlines.

The authors acknowledge financial support from the EU design study SAXIER (RIDS contract No. 011934) and are grateful to V. Lamzin and C. Betzel for providing the MAR345 detector.

References

Benoit, E., Chovin, A., Foulloy, L., Chatenay, A. & Mauris, G. (2006). *IEEE Trans. Instrum. Meas.* **55**, 771–777.
Berry, A., Helsby, W. I., Parker, B. T., Hall, C. J., Buksh, P. A., Hill, A., Clague, N., Hillon, M., Corbett, G., Clifford, P., Tidbury, A., Lewis, R. A., Cernik, B. J., Barnes, P. & Derbyshire, G. E. (2003). *Nucl. Instrum. Methods A*, **513**, 260–263.
Boulin, C. J., Kempf, R., Gabriel, A. & Koch, M. H. J. (1988). *Nucl. Instrum. Methods A*, **269**, 312–320.
Cena, G., Valenzano, A. & Vitturi, S. (2001). *Int. J. Comput. Integr. Manuf.* **14**, 41–54.
Dubuisson, J.-M., Decamps, T. & Vachette, P. (1997). *J. Appl. Cryst.* **30**, 49–54.
Farsi, M. & Ratcliff, K. (1998). *IEEE Rev.* **44**, 229–231.
Gherardi, E., Sandin, S., Petoukhov, M. V., Finch, J., Youles, M. E., Ofverstedt, L. G., Miguel, R. N., Blundell, T. L., Vande Woude, G. F., Skoglund, U. & Svergun, D. I. (2006). *PNAS*, **103**, 4046–4051.
Hammersley, A. P. (1998). Report ESRF98HA01T. ESRF, Grenoble, France.
Koch, M. H. J. & Bordas, J. (1983). *Nucl. Instrum. Methods*, **208**, 461–469.
Konarev, P. V., Petoukhov, M. V., Volkov, V. V. & Svergun, D. I. (2006). *J. Appl. Cryst.* **39**, 277–286.
Lawrenz, W. (1997). CAN (Controller Area Network). Heidelberg: Huethig.
Nakamura, Y., Akashi, K., Norisuye, T., Teramoto, A. & Sato, M. (1997). *Polym. Bull.* **38**, 469–476.
Petoukhov, M. V., Konarev, P. V., Kikhney, A. G. & Svergun, D. I. (2007). *J. Appl. Cryst.* **40**, s223–s228.
Petoukhov, M. V. & Svergun, D. I. (2003). *J. Appl. Cryst.* **36**, 540–544.
Plaisier, J. R., Koning, R. I., Koerten, H. K., van Roon, A. M., Thomassen, E. A. J., Kuil, M. E., Hendrix, J., Broennimann, C., Pannu, N. S. & Abrahams, J. P. (2003). *Nucl. Instrum. Methods*, **509**, 274–282.
Svergun, D. I. & Koch, M. H. J. (2003). *Rep. Prog. Phys.* **66**, 1735–1782.
Vestergaard, B., Sanyal, S., Roessle, M., Mora, L., Buckingham, R. H., Kastrup, J. S., Gajhede, M., Svergun, D. I. & Ehrenberg, M. (2005). *Mol. Cell*, **20**, 929–938.
Zeltwanger, H. (2001). CANopen. Berlin: VDE Verlag.